



Numerical Analysis of Settlement-Induced Damage to a Masonry Church Nave Wall

Leidy Bejarano-Urrego¹, Els Verstrynge¹(✉), Anastasios Drougkas¹,
Giorgia Giardina², Maarten Bassier³, Maarten Vergauwen³,
and Koen Van Balen¹

¹ Building Materials and Technology, Civil Engineering Department,
KU Leuven, Leuven, Belgium
{leidyelvira.bejaranourrego, els.verstrynge,
anastasios.drougkas, Koenraad.vanbalen}@kuleuven.be
² Department of Architecture and Civil Engineering,
University of Bath, Bath, UK
G.Giardina@bath.ac.uk
³ Geomatics Research Group, KU Leuven, Ghent, Belgium
{maarten.bassier, maarten.vergauwen}@kuleuven.be

Abstract. Differential soil settlements can induce structural damage to heritage buildings, causing not only economic but also cultural value losses. In 1963, the Saint Jacob's church in Leuven was permanently closed to the public because of severe settlement-induced damage caused by insufficient bearing capacity of the foundation. Currently, the church is stabilized using a temporary shoring system. This work aims at implementing a practical modelling approach to predict damage on church nave walls subjected to differential settlements. For that purpose, a finite element model of the Saint Jacob's church nave was generated and validated through on-site monitoring data including levelling, damage survey and laser scanning. The model takes into account the non-linear behavior of the masonry by means of continuum smeared cracking. The paper introduces two approaches to model the settlement on the structure. One of them consists in the direct application of vertical displacements underneath the structure according to the deformation profile measured on-site. In the second approach, interfaces with different stiffness are placed at the base allowing the structure to deform under its self-weight. In addition, the effect of the settlement profile type in the damage level is analyzed.

Keywords: Differential settlements · Crack patterns · FE modelling
Damage surveying · Case study

1 Introduction

The Saint Jacob's church is a three-nave church located in Leuven, Belgium (Fig. 1). It was turned into an early Gothic style church through several construction phases. The original Romanesque bell tower dates back to 1220, the naves, transept and chapels were built from the 13th to the 16th century and the neoclassical choir was built in the 18th century. The church is located on a compressible sandy clay soil with limited load-

bearing capacity. The original foundation system was not designed for the load that was later added, causing large differential settlements and subsequent damage. Schueremans et al. [1] compiled all the structural assessments and consolidation measures performed on the church up to 2005, including historic and damage surveys, material characterization, settlement monitoring, structural analysis, diagnosis and intervention proposals.



Fig. 1. Saint Jacob's church (a), view of main nave with choir in the back, in 1918 (b) and 2016 (c)

One of the most critical construction phases occurred at the turn of the 15th to 16th century when the walls on the main nave were heightened by approximately 8.4 m and the wooden roof was replaced by brick vaults with a thickness of 22 cm [2]. This overloading would trigger new differential settlements, estimated up to 10 cm [1]. Different stability assessments and restoration works took place from the 15th century onward. In 1963, the church was permanently closed to the public due to overall stability problems. The vaults in the aisles were thereupon dismantled and a steel shoring system was inserted to relieve the columns of the nave (Fig. 1c). Concrete frames were placed to stabilize the structure. In 1999–2000, the flying buttresses were dismantled because of their severe deformation and replaced by tie-rods to ensure stability [2, 3]. In addition, since the church has been out of service since 1963, important deterioration has occurred over time.

This work specifically investigates the mechanical behavior of one of the main nave walls of the church, which has been severely cracked due to differential settlements (Fig. 2). In the literature, several numerical assessment methodologies to model settlement-induced damage on masonry have been proposed [4–6]. The current methodology investigated in this paper includes two simplified non-linear numerical models, considering as input the settlement profile that was measured on-site. The absence of on-site measurements may be complemented by satellite data [7]. They are validated through comparison with a damage survey. A second objective of this paper is the assessment of the structural damage in terms of cracking as a function of the settlement profile.

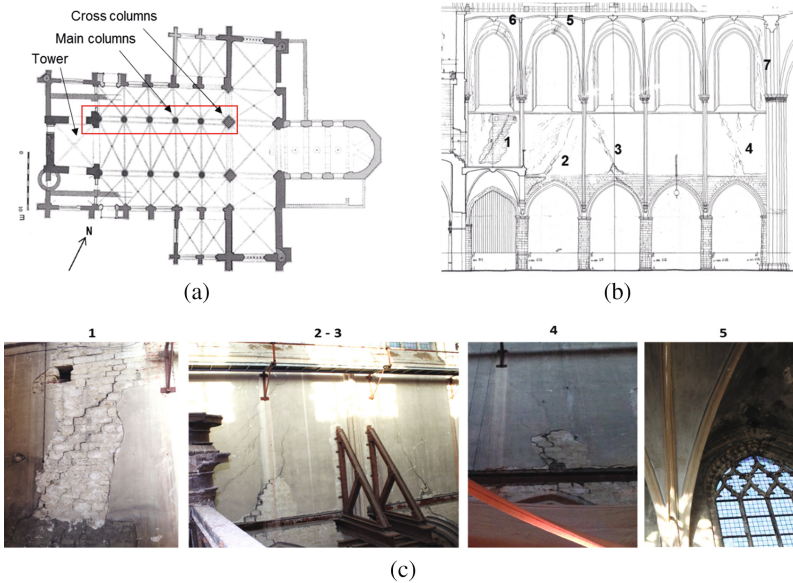


Fig. 2. Analyzed nave wall, plan view (a), crack pattern (b) and photographic survey (c). The numbering of the cracks on the crack pattern (b) corresponds to the pictures presented in (c)

2 Site Investigation

The main structural problems of Saint Jacob’s church originated from a lack of load-bearing capacity of the foundation, which is built on compressible sandy clay soil. Investigations in pits, dug underneath different columns, allowed to identify the foundation system, which is composed of enlarged masonry pillars made of regular blocks of natural stone and lime mortar joints. The depth of the foundation pillars under the current floor level is about 2.9 and 3.7 m for the main and cross columns, respectively. In addition, decayed wooden elements were found underneath the pillars, placed 1.6 m below the water table. After a rigorous assessment, Schueremans et al. [1] concluded that the foundation system did not fulfill the required load-bearing capacity causing severe differential settlements. This system was not originally designed for the self-weight increase of the church over time. In addition, these settlements intensified as a consequence of the decayed wooden elements underneath the foundation pillars, which might have caused the pillars to be punched into the subsoil.

The wall that is analyzed in this paper is the severely cracked northern wall of the main nave (Fig. 2a). The damage pattern is shown in Fig. 2b, c. This crack pattern is mainly caused by the settlement of the nave columns. The vertical displacements of the cross columns as well as the tower are significantly smaller than those of the columns in the nave. As a result, diagonal cracking appears in the masonry wall above the arcade similarly to shear cracking in a simply supported beam, with supports on the cross columns and tower.

Two levelling surveys have been performed on the building [1, 8]. Relative displacements measured in 1994 and 2005 at the base of the columns and walls indicate a maximum differential settlement of 9.3 mm across the structure during the measurement interval of 11 years. The corresponding relative displacement profile of the nave columns with respect to the cross column is shown in Fig. 3 (1. Displacement profile). It presents a maximum settlement of 6 mm under the second column (counted from the left) in the period 1994–2005. However, it is important to notice that according to the crack pattern indicated in Fig. 2b, it seems that the third column might have accumulated the largest vertical displacement during the lifetime of the masonry wall.

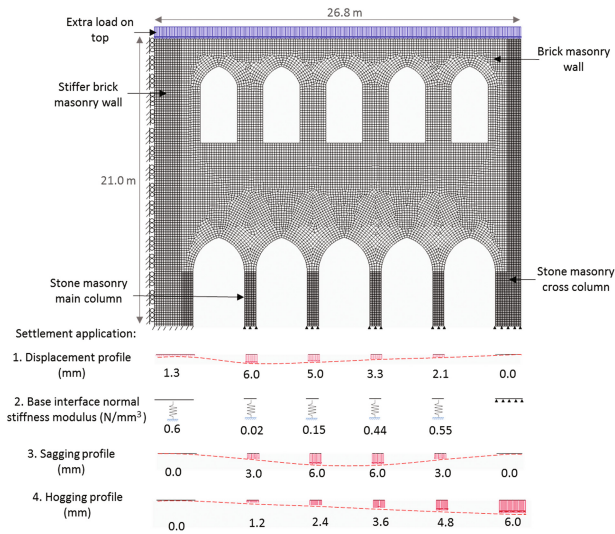


Fig. 3. Model of the nave wall with applied settlement profiles and interface stiffness values

The nave wall is made of brick masonry with a thickness of 0.85 m. The cross and main columns are made of sandstone masonry with cross sections of 1.69 and 0.54 m², respectively. Some of the mechanical properties of the brick, stone as well as mortar were measured from several core samples [1, 9]. They are shown in Table 1.

Table 1. Mechanical properties for the numerical model.

Mechanical properties		Brick masonry	Stone masonry
Compressive strength	f_c (MPa)	<u>6.99</u>	<u>11.95</u>
Modulus of elasticity	E (MPa)	3000	<u>15700</u>
Poisson's ratio	ν	0.15	<u>0.2</u>
Tensile strength	f_t (MPa)	0.1	1.0
Fracture energy	G_t (N.mm/mm ²)	0.012	0.075
Density	ρ (kg/m ³)	<u>1920</u>	<u>2360</u>

Note: Underlined values are taken from testing campaigns [1, 9]

3 Numerical Modeling

3.1 Pre-processing

A continuum smeared cracking strategy was implemented to model the settlement-induced damage on the nave wall. Within this strategy, bricks, mortar and brick-mortar interfaces are smeared out in a homogeneous continuum composite. A multi-directional fixed crack model was adopted, in which cracking is specified as a combination of tension cut-off, linear tension softening and full shear retention [10, 11]. The tension softening law is defined by the tensile strength of the composite masonry f_t , the tensile fracture energy G_f , and the crack bandwidth h , which is assumed equal to 166 mm (about the size of the element side). The nave wall was modelled using 8-node quadrilateral plane stress elements with 2×2 Gaussian integration points. A comparison between smeared and discrete cracking models for accurately modelling crack widths in masonry was presented in [12].

The numerical model is shown in Fig. 3. The extra load on top represents the roof, the main vault and the non-structural elements, having a load value of 7.6 kN/m [9]. The nave wall model is composed of a 850 mm thick brick masonry wall, 740 mm thick stone masonry main columns, a 1300 mm thick stone masonry cross column and a stiffer brick masonry wall on the side with a thickness of 2000 mm. The mechanical properties of the materials are shown in Table 1. The underlined properties were taken from testing campaigns [1, 9]. The tensile strength of the stone masonry was assumed equal to 1.0 MPa (about 10% of the compressive strength). The rest of the values were taken from literature [4, 13–15].

Two approaches for the settlement application were considered. Approach 1 consists in the direct application of vertical displacements in the nodes underneath the structure, equal to the deformation profile measured on-site, as schematically indicated in Fig. 3 (1. Displacement profile). In this approach, the displacements induced by the self-weight and extra dead load were reset to zero. Then, the displacement profile was applied in 50 steps, so that the damage evolution could be easily tracked until it reached the maximum displacement value, for instance 6.0 mm under the second column.

In approach 2, interfaces with different stiffness values were placed at the base nodes, allowing the structure to deform under its self-weight. The normal stiffness values for the interface were obtained after a calibration procedure, which consisted in the variation of the stiffness values to match a base deformation profile similar to the profile measured on-site. The final values are indicated in Fig. 3 (2. Base interface normal stiffness modulus). In this approach, the self-weight and extra dead load were applied in 50 load steps and the vertical displacement at the base was monitored after each load increment. The possibility for the structure to deform according to its self-weight makes this approach more realistic. However, the selection of the normal stiffness modulus values is not straightforward, and a set of values that differ in orders of magnitude from each other might be required. For instance, in this case a very low value (0.02 N/mm^3) was applied under the column that presented the maximum vertical displacement. The ratio between the normal and shear stiffness modulus typically ranges from 2.18 to 2.5 [16]; for the current study, this ratio was assumed equal to 2.4.

3.2 Influence of the Settlement Application Mode

Figure 4 shows the results of the models in terms of the crack pattern at the final step of the numerical analysis. Both approaches match well throughout the entire analysis, suggesting the ability of both to accurately simulate settlement-induced cracking. They both captured the main cracks observed in the damage survey (cracks 1 to 5 in Fig. 2). However, the location of some of them is slightly shifted, for instance cracks 1 and 4 appear from the external corner of the windows rather than from the internal corner as shown in the damage survey.

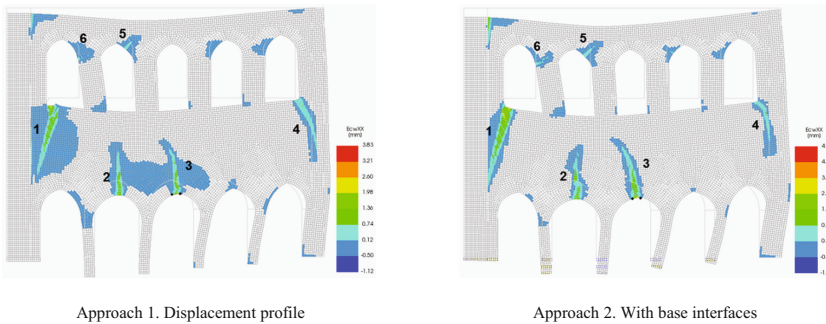


Fig. 4. Final deformed mesh and crack pattern indicating crack width

Approach 1 shows a lower maximum vertical displacement at the top of the wall than approach 2, with values of 3.9 mm and 5.8 mm respectively. This occurs because in approach 2, the loading (self-weight and extra load) acts uniformly on the entire structure, in contrast to approach 1 in which the applied vertical displacement is localized only at the base. This phenomenon might cause local stress concentrations and additional minor cracks when using approach 1.

Figure 5 shows the width of crack 3, located on top of the middle arch, in terms of the maximum vertical displacement at the base of the second column, which presents the highest displacement. This crack width was calculated as the horizontal separation of the nodes indicated with black dots in Fig. 4. Even though approach 2 considers a very low normal stiffness at the base of the second column, the vertical displacement did not reach 6.0 mm but only 5.1 mm. The model still exhibits a larger crack width, up to 4.9 mm. Approach 1 induces a maximum crack width of 3.4 mm. Although the crack patterns present very good agreement with the on-site crack survey, the actual crack widths could not be validated as no crack width measurements were done and the initial deformations in 1994 (reference levelling measurement) are unknown.

3.3 Influence of Settlement Profile Type

Considering approach 1, different settlement profiles were applied at the base of the structure, to evaluate their influence on the structure response. First, a sagging effect was considered, in which the profile is symmetric and the maximum settlement takes

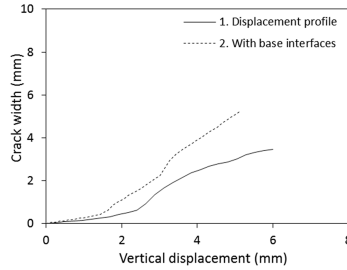


Fig. 5. Width of crack 3 as a function of maximum vertical displacement at the column base

place in the middle of the structure, as indicated in Fig. 3 (3. Sagging profile). Second, a hogging profile was applied, which considers a non-symmetrical linear settlement profile having the maximum displacement at the base of the cross column on the right, as shown in Fig. 3 (4. Hogging profile).

Figure 6 shows the deformed mesh and crack pattern for the sagging and hogging profiles when reaching the maximum applied vertical displacement of 6.0 mm. The sagging settlement profile causes the middle arch to open with a large crack in the middle top (4.1 mm wide) as a result. The hogging profile induces cracks on the left part of the nave wall, next to the stiffer masonry wall. It seems that the crack pattern acts as a hinge, where the right part rotates clockwise around the crack tip. The crack width obtained with this profile type is lower (the indicated crack is 2.3 mm wide).

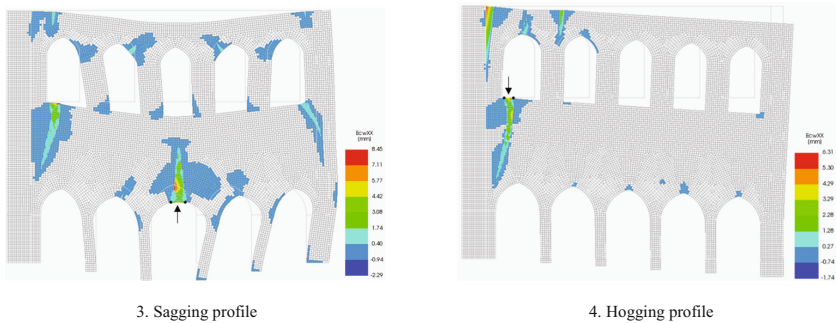


Fig. 6. Deformed mesh and crack pattern indicating crack width for sagging and hogging

Figure 7 shows the width evolution of the marked cracks as a function of the maximum vertical displacement at the base for both profile types. It also shows the width of crack 3 obtained with the measured settlement profile (1. Displacement profile). Extra analysis steps were performed to proportionally apply the double settlement profiles at the base up to a maximum settlement of 12 mm. The most critical situation occurred with the sagging profile in which the crack width went up to 9.7 mm. In the hogging profile, the crack width reached 4.6 mm. The crack width for the measured profile remained in between throughout the analysis.

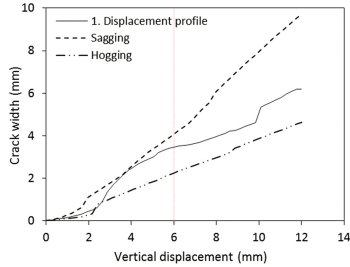


Fig. 7. Crack width as a function of the maximum vertical displacement at the base

4 Remarks and Conclusions

This paper presented two approaches to model settlement-induced damage on a church nave wall, knowing the settlement profile measured in levelling surveys. Approach 1 consisted in the direct application of the measured vertical displacements. In approach 2, interfaces with different normal stiffness were placed underneath the structure allowing deformation only under its self-weight. Even though approach 2 might be more realistic because there is no need to apply extra vertical displacements in the nodes, the selection of the normal stiffness modulus values is not straightforward. In approach 1, the damage can be tracked easily after each deformation increment. Both approaches matched well to the observed damage, suggesting the ability of both to accurately simulate settlement-induced cracking. Finally, the effect of different settlement profiles, sagging and hogging type, was analyzed. Results show that the sagging profile induced the largest cracks, located at the middle arch. Future work will focus on an extension towards time-dependent models to include the full history of the church.

Acknowledgments. This work was done within the framework of the GEPATAR project (“GEotechnical and Patrimonial Archives Toolbox for ARchitectural conservation in Belgium” BR/132/A6/Gepatar), supported by BRAIN.be, Belspo.

References

1. Schueremans L, Van Balen K et al (2007) The church of Saint James at Leuven: structural assessment and consolidation measures. *Int J Archit Herit* 1:82–107
2. Verstrynghe E, Schueremans L, Smars P (2012) Controlled intervention: monitoring the dismantlement and reconstruction of the flying buttresses of two Gothic churches. *Int J Archit Herit* 6:689–708
3. Smars P, Schueremans L, Van Balen K (2006) Monitoring of dismantlement of four flying buttresses. In: *Structural analysis of historical constructions*. New Delhi
4. Giardina G (2013) Modelling of settlement induced building damage. PhD thesis, TU Delft
5. Camós C (2015) Sensitivity of urban buildings to tunneling-induced settlements. PhD Thesis, Universitat Politècnica de Catalunya, Barcelona, p 167

6. Burd HJ, Houlsby GT, Augarde CE, Liu G (2000) Modelling tunnelling-induced settlement of masonry buildings. In: Proceedings of the institution of civil engineers - geotechnical engineering, pp 17–19
7. Tomás R, García-Barba J et al (2012) Subsidence damage assessment of a Gothic church using differential interferometry and field data. *Struct Health Monit* 11:751–762
8. Schueremans L, Van Balen K et al (2006) Hydrostatic levelling system – monitoring of historical structures. In: Lourenço PB et al (eds) *Structural analysis of historical constructions*. New Delhi
9. Sanchez-Beitia S, Schueremans L, Van Balen K (2009) On-site stress measurement on the piers of the Saint Jacobs church in Leuven, Belgium. *Int J Archit Herit* 3:110–125
10. TNO (2016) DIANA Finite Element Analysis, User’s Manual. In: Manie J, Kikstra WP (eds) *TNO DIANA BV*
11. Lourenço PB (1996) Computational strategies for masonry structures. PhD Thesis, TU Delft
12. Bejarano-Urrego L, Verstrynghe E, Giardina G, Van Balen K (2018) Crack growth in masonry: numerical analysis and sensitivity study for discrete and smeared crack modelling. *Eng Struct* 165:471–485
13. Rots JG (1997) Structural masonry-an experimental/numerical basis for practical design rules. TNO Building and Construction Research, A.A Balkema, N. Rotterdam
14. Drougkas A (2015) Derivation of the properties of masonry through micro-modeling techniques. PhD thesis, Polytechnic University of Catalonia, Barcelona
15. Van der Pluijm R (1993) Shear behavior of bed joints. In: Hamid A, Harris H (eds) *6th North American masonry conference at Drexel university, Philadelphia*, pp 125–136
16. Sarhosis V, Sheng Y (2015) Identification of material parameters for low bond strength masonry. *Eng Struct* 60:100–110